INORGANIC CHEMISTRY

FRONTIERS

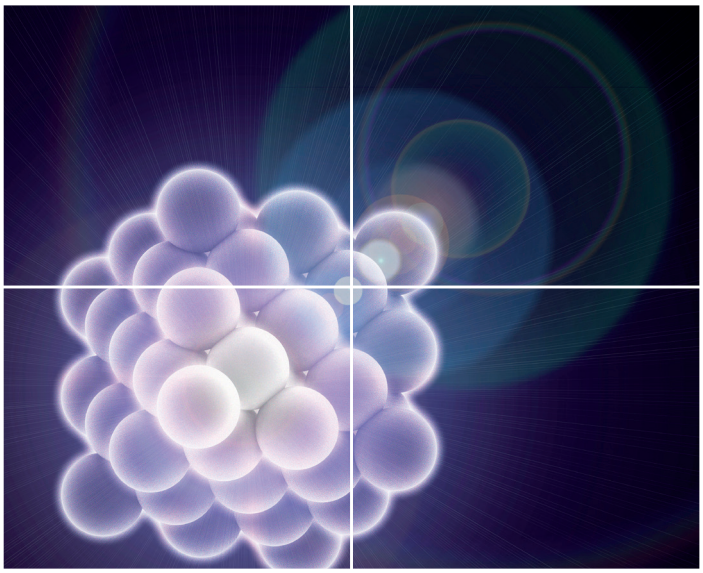

Accepted Manuscript

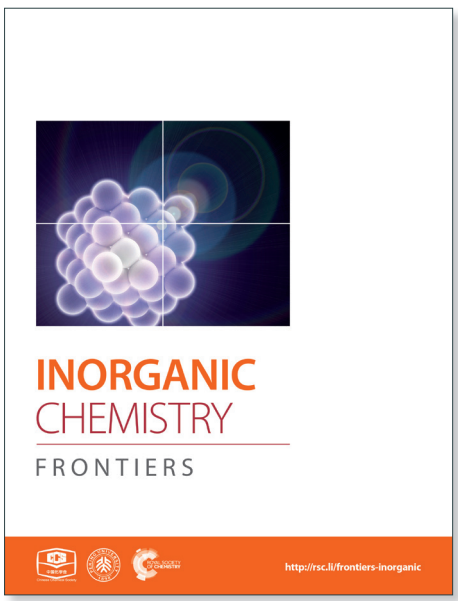

This is an *Accepted Manuscript*, which has been through the Royal Society of Chemistry peer review process and has been accepted for publication.

Accepted Manuscripts are published online shortly after acceptance, before technical editing, formatting and proof reading. Using this free service, authors can make their results available to the community, in citable form, before we publish the edited article. We will replace this *Accepted Manuscript* with the edited and formatted *Advance Article* as soon as it is available.

You can find more information about *Accepted Manuscripts* in the **Information for Authors**.

Please note that technical editing may introduce minor changes to the text and/or graphics, which may alter content. The journal's standard **Terms & Conditions** and the **Ethical guidelines** still apply. In no event shall the Royal Society of Chemistry be held responsible for any errors or omissions in this *Accepted Manuscript* or any consequences arising from the use of any information it contains.

Inorganic anion-assisted supramolecular assemblies of bent dipyridines: effects of anionic geometries on the hydrogen-bonding networks

Xue-Hua Ding[a], Shi Wang[a]*, Yong-Hua Li[a]* and Wei Huang[ab]

[a] *Key Laboratory for Organic Electronics & Information Displays (KLOEID) and Institute of Advanced Materials (IAM), , National Synergistic Innovation Center for Advanced Materials (SICAM), Nanjing University of Posts & Telecommunications, Nanjing 210023, China*

[b] *Key Laboratory of Flexible Electronics (KLOFE) & Institute of Advanced Materials (IAM), National Synergistic Innovation Center for Advanced Materials (SICAM), and Institute of Advanced Materials, Nanjing Tech University, Nanjing 211816, China*

** Corresponding authors. Tel/Fax: +86 25 85866396 (S. Wang); +86 25 85866332 (Y.-H. Li); +86 25 85866008 (W. Huang)*

E-mail addresses: iamswang@njupt.edu.cn (S. Wang), iamyhli@njupt.edu.cn (Y.-H. Li)

A series of inorganic acids were introduced into the self-assembly with the bent 2,5-bis(4-pyridyl)-1,3,4-oxadiazole (4-bpo), yielding seven anion-assisted supramolecular salts, *i.e.* $[(4\text{-}H_2bpo^{2+})\ (NO_3^-)_2]\cdot 2H_2O$ (**1**), $(4\text{-}H_2bpo^{2+})\ (HPO_4^{2-})$ (**2**), $[(4\text{-}H_2bpo^{2+})_2\ (4\text{-}Hbpo^{+})\ (I_3^-)_3\ (I^-)_2]\cdot 2H_2O$ (**3**), $[(4\text{-}Hbpo^{+})_2\ (PF_6^-)_2]\cdot H_2O$ (**4**), $[(4\text{-}H_2bpo^{2+})\ (BF_4^-)_2]\cdot H_2O$ (**5**), $[(4\text{-}Hbpo^{+})\ (BF_4^-)]$ (**6**) and $(4\text{-}H_2bph^{2+})\ (SO_4^{2-})$ (**7**). Structural analyses indicate that different inorganic anions (*e.g.* spherical, linear, trigonal planar, tetrahedral and octahedral) can induce the formation of diverse supramolecular architectures, influencing the crystallization ratio, the protonated number and the final structures. The anions are hydrogen bonded to the angular dipyridine, which offers a sufficient driving force for the directed assembly of

supramolecular hydrogen-bonding frameworks. Thereinto, various hydrogen-bonding motifs are observed in all these cases (**1**–**7**) and the nitrogen atoms of pyridines are protonated other than salt **6**. Among them, salts **1**, **3**, **4** and **5** crystallize with water molecules but others do not. Interestingly, appealing substructures have been generated by anions and water molecules in **1**, **3** and **5** except **4**, while HPO_4^{2-} dimers form in **2** despite no assist by the solvent water. BF_4^- anions facilitate the formation of the helical chain in **6**. Unexpectedly, the oxadiazole ring opened *via* the in situ hydrolysis under hydrothermal conditions during crystallization with H_2SO_4, producing salt **7**.

Introduction

Inspired by the fundamental and vital roles of ubiquitous anions in the areas of chemistry, biology, medicine and environmental issues, an upsurge in anion supramolecular chemistry is witnessed in the past few decades.[1-10] However, since the crystallization process will be complicated by its high charge density[11] and the formation of hydrogen bonds and anion···π interactions are unforeseeable,[12] the strategy of inorganic anions used for the synthesis of supramolecular architectures remains underdeveloped.[1, 10, 13-21] By serendipitous discoveries, anions have proven their ability to control supramolecular assemblies by interacting with their receptors, such as hydrogen-bonding, electrostatic and anion···π interactions.[11, 22-27]

Therefore, worldwide chemists do their endeavor to tackle the challenges posed by anions nowadays and the systematic research on the structural variations and physicochemical properties of supramolecular arrays are increasingly being pursued based on inorganic anions and their receptors.[28-35] From a structural point of view, anions may play various roles in dynamic crystallization process, for instance, acting as a structure-directing agent, a spectator merely for charge balance, building unit and secondary building unit (SBU).[11] The final structures can be effectively influenced by the nature and geometry of inorganic anions, such as spherical (halides), linear (triiodide), coplanar (carboxylate), trigonal planar (nitrate), tetrahedral (sulfate) and octahedral (hexafluorophosphate).[6, 12, 13]

Intermolecular non-covalent interactions facilitate the process of supramolecular assembly between anions and their receptors with functional groups. Currently, multifarious novel artificial anion receptors have emerged, ranging from amide/urea, pyrrole/indole, guanidinium, polyammonium, calix[n]phyrins, imidazolium to pyridine/pyridinium.[36, 37] Among them, we have reported the supramolecular salts based on bent dipyridyl 2,2'-dipyridylamine (dpa) as a proton sponge[38] and have an ongoing interest in appealing angular dipyridyl 2,5-bis(4-pyridyl)-1,3,4-oxadiazole (4-bpo). The relatively flexible conformation can induce higher-dimensional supramolecular architectures more easily compared with that in linear dipyridyl derivatives.[39] Furthermore, protonation or quaternization occurs readily in the pyridine heterocycles, resulting in pyridinium groups which can interact with anions through a range of noncovalent interactions such as electrostatics, increasingly polarized hydrogen bonds (including CH···A^-) or electrostatic aryl–aryl stacking interactions.[36]

Although Du *et al.* introduced 4-bpo to a series of organic acids to construct supramolecular crystalline materials,[39-43] the systematic research has not been carried out on the system of inorganic acids except two discrete ionic salts.[44, 45] Herein, we synthesized seven inorganic anion-assisted supramolecular salts (Scheme 1), namely $[(4\text{-}H_2bpo^{2+})\ (NO_3^-)_2]\cdot 2H_2O$ (**1**), $(4\text{-}H_2bpo^{2+})\ (HPO_4^{2-})$ (**2**), $[(4\text{-}H_2bpo^{2+})_2\ (4\text{-}Hbpo^+)\ (I_3^-)_3\ (I^-)_2]\cdot 2H_2O$ (**3**), $[(4\text{-}Hbpo^+)_2\ (PF_6^-)_2]\cdot H_2O$ (**4**), $[(4\text{-}H_2bpo^{2+})\ (BF_4^-)_2]\cdot H_2O$ (**5**), $[(4\text{-}Hbpo^+)\ (BF_4^-)]$ (**6**) and $(4\text{-}H_2bph^{2+})\ (SO_4^{2-})$ (**7**). The variation of anions has directed entirely different supramolecular architectures, diverse hydrogen-bonding motifs and interesting substructures with water. Meanwhile, hydrothermal conditions show control over the crystallization process, such as the change of protonated site in salt **6** and the hydrolysis of 4-bpo in **7**. It is extremely rare that the oxadiazole is protonated except only one case[46] when diazole and pyridine rings coexist according to the Cambridge Structure Database (CSD).

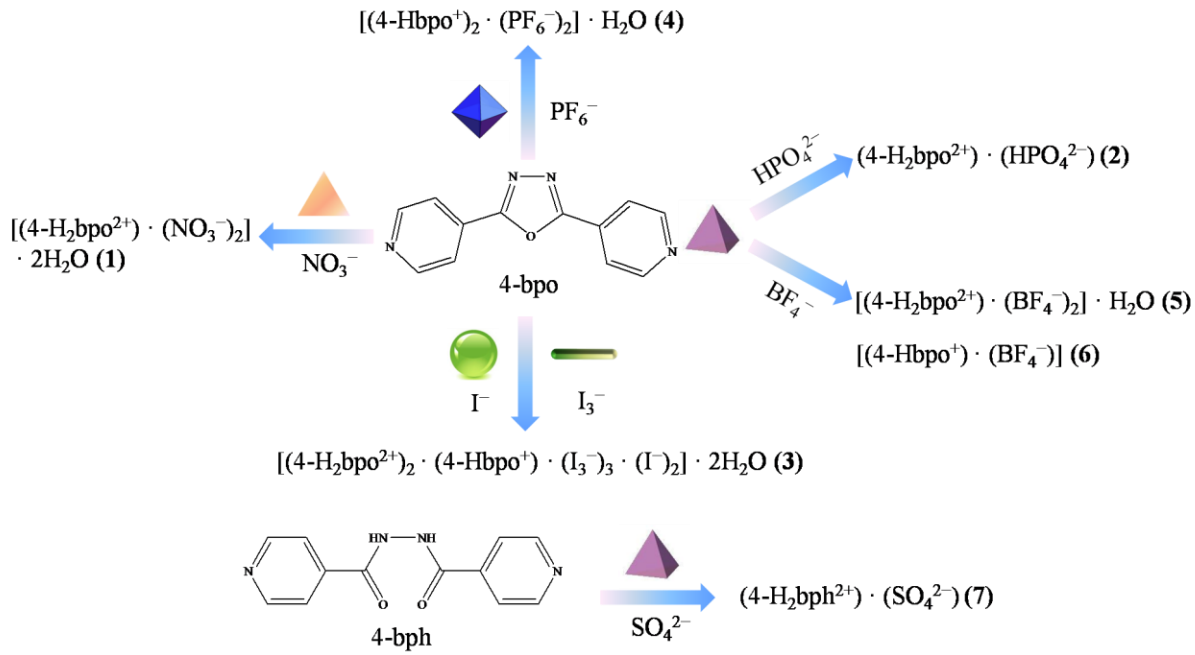

Scheme 1 Proton-transfer supramolecular salts (**1**–**7**) form, induced by different geometrical anions (spherical, linear, trigonal planar, tetrahedral and octahedral).

Experimental

Syntheses of the compounds 1–7

4-Bpo was prepared according to the literature procedures,[47] and other chemical reagents and solvents (analysis grade) were commercially available (Sigma-Aldrich) and used without further purification.

[(4-H_2bpo^{2+}) (NO_3^-)$_2$] 2H_2O (1). To a methanol solution (5 mL) containing 4-bpo (0.1 mmol) was added aqueous solution (5 mL) of HNO_3 (0.2 mmol) with constant stirring for 30 mins. The resultant clear solution was allowed to evaporate under ambient conditions, affording colorless needle-shaped crystals after one week. The crystals were separated from the mother liquor by filtration, washed with cool methanol solution, and dried under vacuum.

(4-H_2bpo^{2+}) (HPO_4^{2-}) (2). 4-Bpo (0.1 mmol) in methanol (5 mL) and H_3PO_4 (0.1 mmol) in water (5 mL) were mixed with stirring according to the similar procedure for **1**. Upon slow evaporation of the solvents, good-quality colorless rodlike crystals of **2** were obtained after two weeks.

[(4-H_2bpo^{2+})$_2$ (4-Hbpo$^+$) (I_3^-)$_3$ (I^-)$_2$] 2H_2O (3). The same synthetic procedure for **1**

was used except that HNO_3 was replaced by HI, giving yellow lamellar single crystals suitable for X-ray analysis over a period of ten days.

$[(4\text{-}Hbpo^{+})_2(PF_6^{-})_2]\cdot H_2O$ (4). Well-shaped colorless rodlike crystals of **4** were isolated about one week by the similar procedure described for **1**, except with the addition of HPF_6 instead of HNO_3.

$[(4\text{-}H_2bpo^{2+})(BF_4^{-})_2]\cdot H_2O$ (5). Similarly to **1**, a methanol/water (v:v = 1:1, 10 mL) mixture of 4-bpo (0.1 mmol) and HBF_4 (0.2 mmol) was allowed to evaporate at ambient conditions, affording colorless rodlike crystals of **5** after two weeks.

$[(4\text{-}Hbpo^{+})(BF_4^{-})]$ (6). The mixture of 4-bpo (0.1 mmol) and HBF_4 (0.1 mmol) in DMF (10 mL) was placed in a Parr Teflon-lined stainless steel vessel (20 mL) under autogenous pressure, which was heated to 120 ℃ for 48 h and subsequently cooled to room temperature at a rate of 10 ℃/h. Colorless block crystals of **6** were obtained.

$(4\text{-}H_2bph^{2+})(SO_4^{2-})$ (7). A water (10 mL) solution containing 4-bpo (0.1 mmol) and H_2SO_4 (0.1 mmol) was placed in a Parr Teflon-lined stainless steel vessel (20 mL) under autogenous pressure, which was heated to 140 ℃ for 72 h and subsequently cooled to room temperature at a rate of 5 ℃/h. Colorless block crystalline products were collected.

Single crystal X-ray diffraction

Crystal data of **1**–**7** were collected by a Bruker SMART APEX diffractometer employing graphite-monochromated Mo Kα radiation (λ = 0.71073 Å) at 293 K. The data integration and reduction were undertaken with SAINT. The structure was solved by the direct method using SHELXS-97 and all the non-hydrogen atoms were refined anisotropically on F^2 by the full-matrix least-squares technique using the SHELXL-97. Non-H atoms were refined anisotropically using all reflections with $I > 2\sigma(I)$. All H atoms (except for those bound to the N atoms on the pyridine and oxadiazole rings) were placed in calculated positions with fixed isotropic thermal parameters. The hydrogen atoms bonded to the N atoms of the pyridine and oxadiazole rings were located from difference maps. The packing views and the asymmetric units were drawn with DIAMOND (Brandenburg and Putz, 2004) Visual Crystal Structure

Information System Software. Crystallographic data and structure refinement are listed in Table 1.

All the hydrogen atoms

Results and discussion

All the one-step reactions were carried out either in 1:2 or 1:1 molar ratio between the bent dipyridine-based synthon 4-bpo and inorganic acids (HNO_3, H_3PO_4, HI, HPF_6, HBF_4 and H_2SO_4, respectively), affording seven proton-transfer supramolecular salts **1**−**7**. For the preparation of **1**−**5**, inorganic acids were mixed directly with 4-bpo in methanol/water (v:v = 1:1, 10 mL) solution, which were allowed to evaporate at ambient conditions and yield the final crystalline products. During crystallization, proton transferred from acid to the nitrogen atom of pyridines. However, the nitrogen of oxadiazole was protonated by HBF_4 in **6** under solvothermal conditions. Interestingly, besides different protonated sites, these salts were obtained as different two-component ratios. In addition, salts **1**, **3**, **4** and **5** crystallized with water molecules while others did not contain solvent molecules. For compound **7**, hydrothermal reactions made the oxadiazole ring open and produced a new organic compound N,N′-bis(4-picolinoyl) hydrazine (4-bph) from the in situ hydrolysis of 4-bpo during crystallization with H_2SO_4. The schematic representations of salts **1**−**7** are summarized in Scheme 1. Hydrogen-bonding geometries and weak intermolecular interactions are listed in Table S1 and Table S2, respectively.

Structure description of compound 1.

Salt **1** crystallizes in a monoclinic space group $P2_1/c$ with one diprotonated 4-H_2bpo^{2+} cation, two trigonal planar NO_3^- anions and two water molecules in the asymmetric unit (Fig. S1a). Two NO_3^- anions both exhibit five hydrogen bonds with 4-H_2bpo^{2+} cations and H_2O molecules due to their three oxygen atoms as hydrogen-bonding acceptors, which range from strong O–H ··O, N–H ··O to weak C–H ··O hydrogen bonds (H ··A, 1.88–2.56 Å; ∠D–H ··A, 126–175 °) (Fig. 1a and Table S1). Moreover, the N6-containing nitrate anion interacts with the N1-containing pyridine and oxadiazole ring in the same 4-H_2bpo^{2+} molecule through anion ··π interactions, where

the distance are 3.766 and 3.228 Å between the closest oxygen atom and the centroid of the aromatic ring, respectively (Table S2).

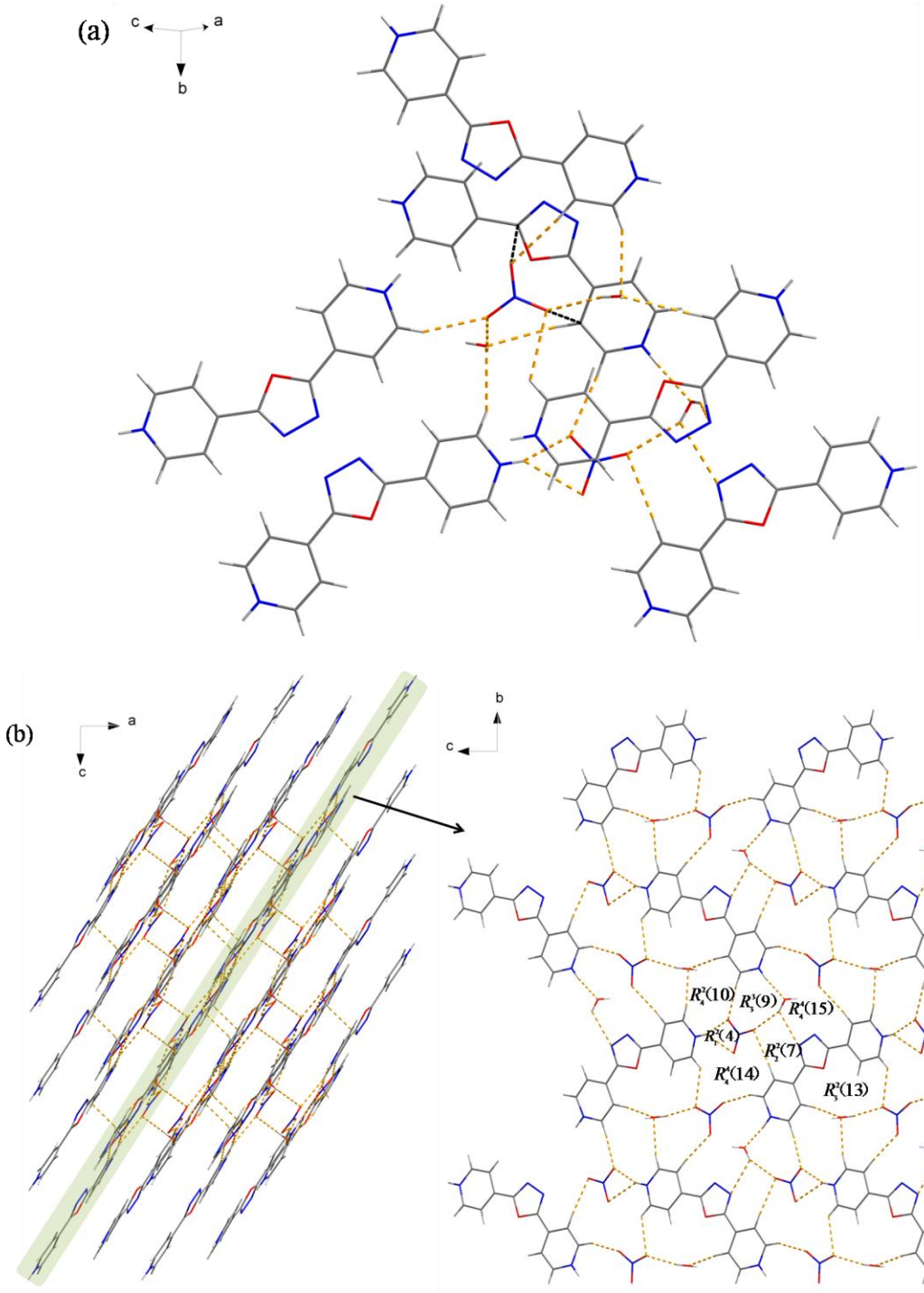

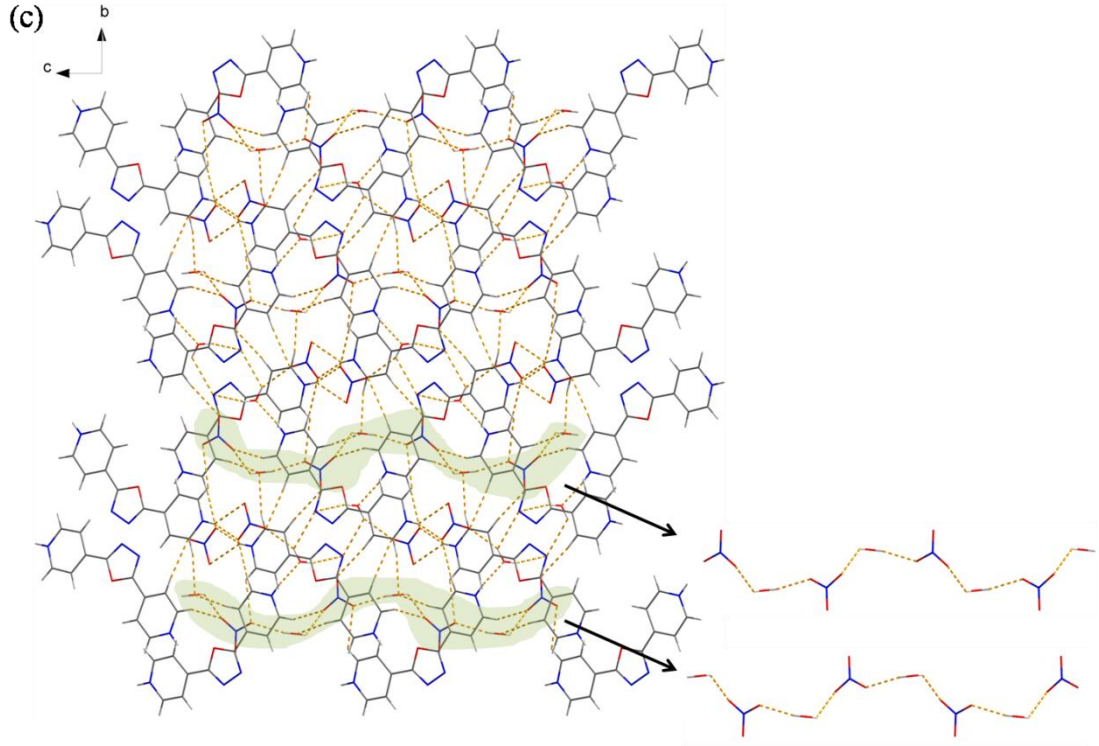

Fig. 1 (a) The coordination sphere of NO_3^- anions in **1**; (b) The 3D hydrogen-bonding network parallel to the *ac*-plane and a side view of the middle chain in pale green viewed along the *a*-axis; (c) The 3D crystal stacking along the *a*-axis and separate molecular structure of NO_3^- anions together with water molecules. Hydrogen bonds and anion$\cdots\pi$ interactions are represented by light orange and black dotted lines, respectively.

Robust and extensive hydrogen-bonding interactions play a crucial role in the crystal packing. Viewed along the *b*-axis, the 4-H_2bpo–nitrate hydrogen-bonding network of **1** is three-dimensional (3D), where parallel chains are connected by O9–H14$\cdots$O7 and O8–H12$\cdots$N2 hydrogen bonds (Fig. 1b). The middle one in pale green has been separated and found as a two-dimensional framework viewed along the *a*-axis, which comprises various ring motifs through robust hydrogen-bonding interactions, *i.e.* $R_1^2(4)$, $R_2^2(7)$, $R_3^3(9)$, $R_4^2(10)$, $R_3^2(13)$, $R_4^4(14)$ and $R_4^4(15)$. Thereinto, 4-H_2bpo^{2+} cations are homo-orientated and parallel to each other in the same layer and every two such layers recur.

When viewed along the *a*-axis, the 3D hydrogen-bonding framework seems not

to be in good order since 4-H_2bpo^{2+}cations are interweaved by NO_3^- anions and water molecules (Fig. 1c). Anions and water are separated in the pale green background and chainlike substructures are observed in antiparallel arrangement. After anions and water molecules have been removed for clarity, we are surprised that no hydrogen-bonding interactions exist among 4-H_2bpo^{2+} cations. But they seem to be wavelike quasi-chains, which in light blue nearly shows mirror symmetry to the adjacent one (Fig. S1b). Even though direct hydrogen-bonding interactions are not involved, cations are guided by NO_3^- anions and H_2O molecules, resulting in the regular structure. It's not hard to see that NO_3^- anion greatly influences the formation of crystal structure.

Structure description of compound 2.

Single-crystal diffraction analysis reveals that **2** crystallizes in the monoclinic space group *C2/c* and its molecular structure is comprised of one diprotonated 4-H_2bpo^{2+} cation and HPO_4^{2-} anion (Fig. S2a). As shown in Fig. 2a, one HPO_4^{2-} anion is bound to four 4-H_2bpo^{2+} cations through N–H$\cdots$O and C–H$\cdots$O hydrogen bonds. Anion$\cdots\pi$ interaction is found between O3 atom and the oxadiazole ring with the distance of 3.440 Å while $\pi\cdots\pi$ interactions are among 4-H_2bpo^{2+} cations (Cg1$\cdots$Cg1 and Cg2$\cdots$Cg3). Notablely, O2 atom can serve as hydrogen-bonding donor as well as acceptor, which facilitates the formation of HPO_4^{2-} dimer *via* strong hydrogen bonds O2–H11$\cdots$O5, notated as $R_2^2(8)$ (Fig. 2b). Such dimers are linked by 4-H_2bpo^{2+} cations *via* strong intermolecular N1–H3$\cdots$O3 and N4–H8$\cdots$O4 hydrogen bonds, offering a large ring $R_6^6(40)$. The four pairs of anions and cations look like a quasi-hexagon viewed along the *b*-axis, which extends to a 3D framework on the *ac*-plane by hydrogen-bonding interactions.

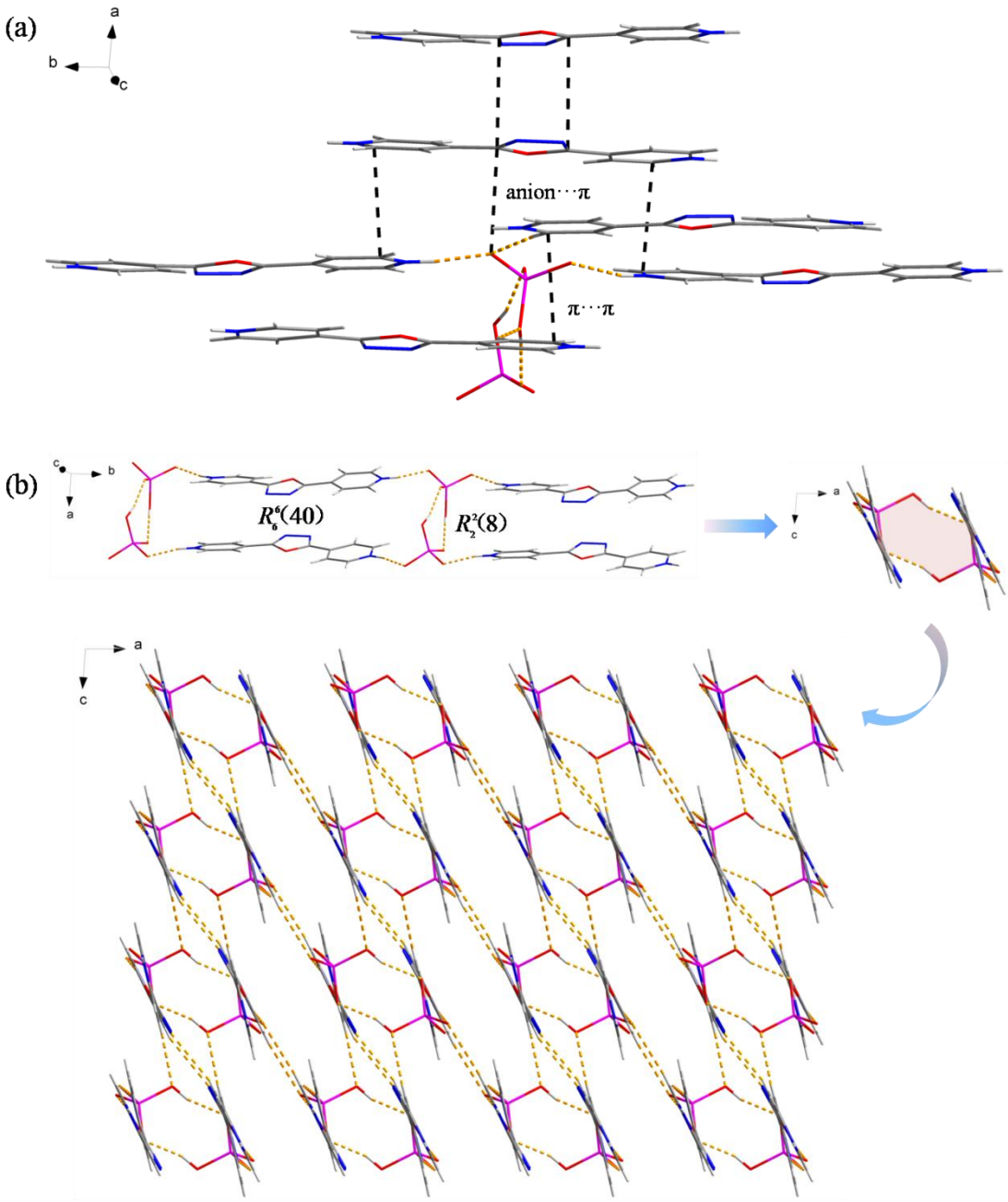

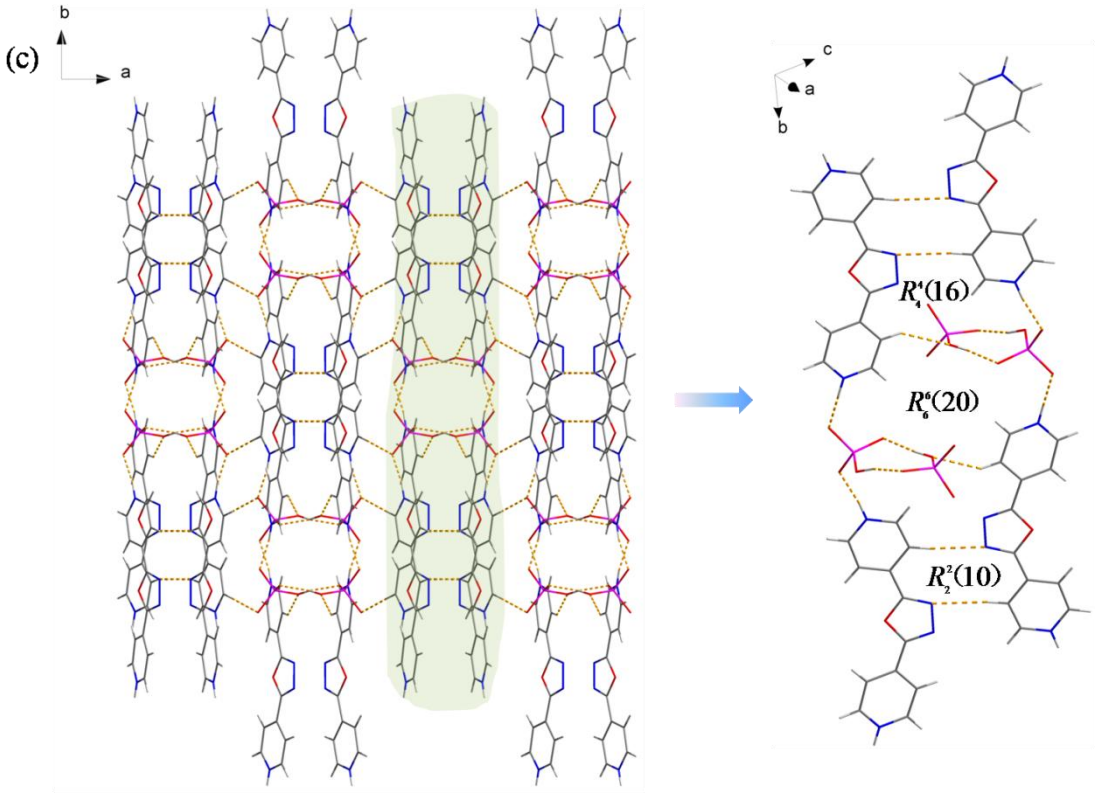

Fig. 2 (a) The coordination sphere of HPO_4^{2-} anion in **2**; (b) A moiety of molecular structure and its stretch on the *ac*-plane into a 3D framework through hydrogen bonds; (c) The 3D crystal stacking along the *c*-axis and a side view of molecular structure in pale green. Hydrogen bonds are represented by light orange dashed lines while anion $\cdots\pi$ and $\pi\cdots\pi$ interactions are black.

From another perspective, it may bring a different scenery. Indeed, as depicted in Fig. 2c, the 4-H_2bpo^{2+}–HPO_4^{2-} hydrogen-bonding framework consists of orderly chains through the weak C2–H2$\cdots$O3 hydrogen bond (H2$\cdots$O3, 2.53 Å; $\angle$ C2–H2$\cdots$O3, 174 °). This indicates that weak hydrogen-bonding interactions also play an important role in the supramolecular assembly. Two groups of HPO_4^{2-} dimers interweave 4-H_2bpo^{2+} cations to show an oval while 4-H_2bpo^{2+} cations are packing to produce a little grid. For clarity, the moiety can be disentangled in pale green and the side view was given on the right. We find the little grid to be a ten-membered ring between two cations owing to C4–H5$\cdots$N2 hydrogen bonds. Other two kinds of large hydrogen-bonding motifs are afforded between anions and cations with the graph-sets

of $R_4^4(16)$ and $R_6^6(20)$.

Structure description of compound 3.

Components in **3** seem slightly richer, which contain two diprotonated 4-H_2bpo^{2+} cations, one monoprotonated 4-Hbpo$^+$ cation, three linear I_3^- anions, two spherical I^- anions and two water molecules in the asymmetric unit (Fig. S3a). As illustrated in Fig. 3a, I10$^-$ and I11$^-$ anions both connect three cations and one H_2O molecule through intermolecular interactions (O–H···I, N–H···I and C–H···I) while three I_3^- anions interact with each other by short I···I contacts (I3···I9, 3.837 Å; I1···I6, 3.922 Å), significantly below the sum of the van der Waals radii of iodine. For cations, $\pi\cdots\pi$ interactions appear (Cg2···Cg1, 3.589 Å; Cg7···Cg4^i, 3.400 Å).

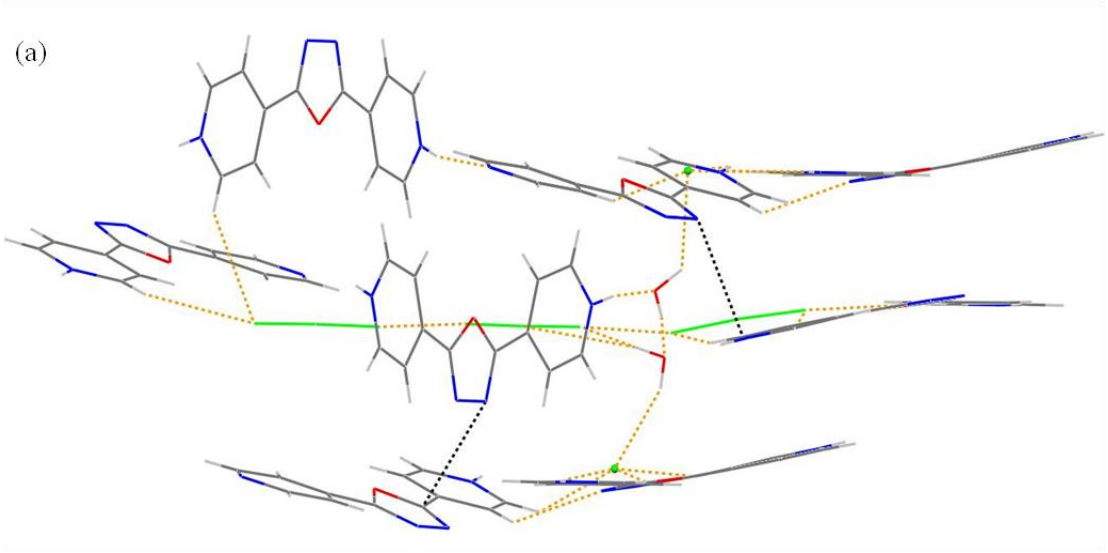

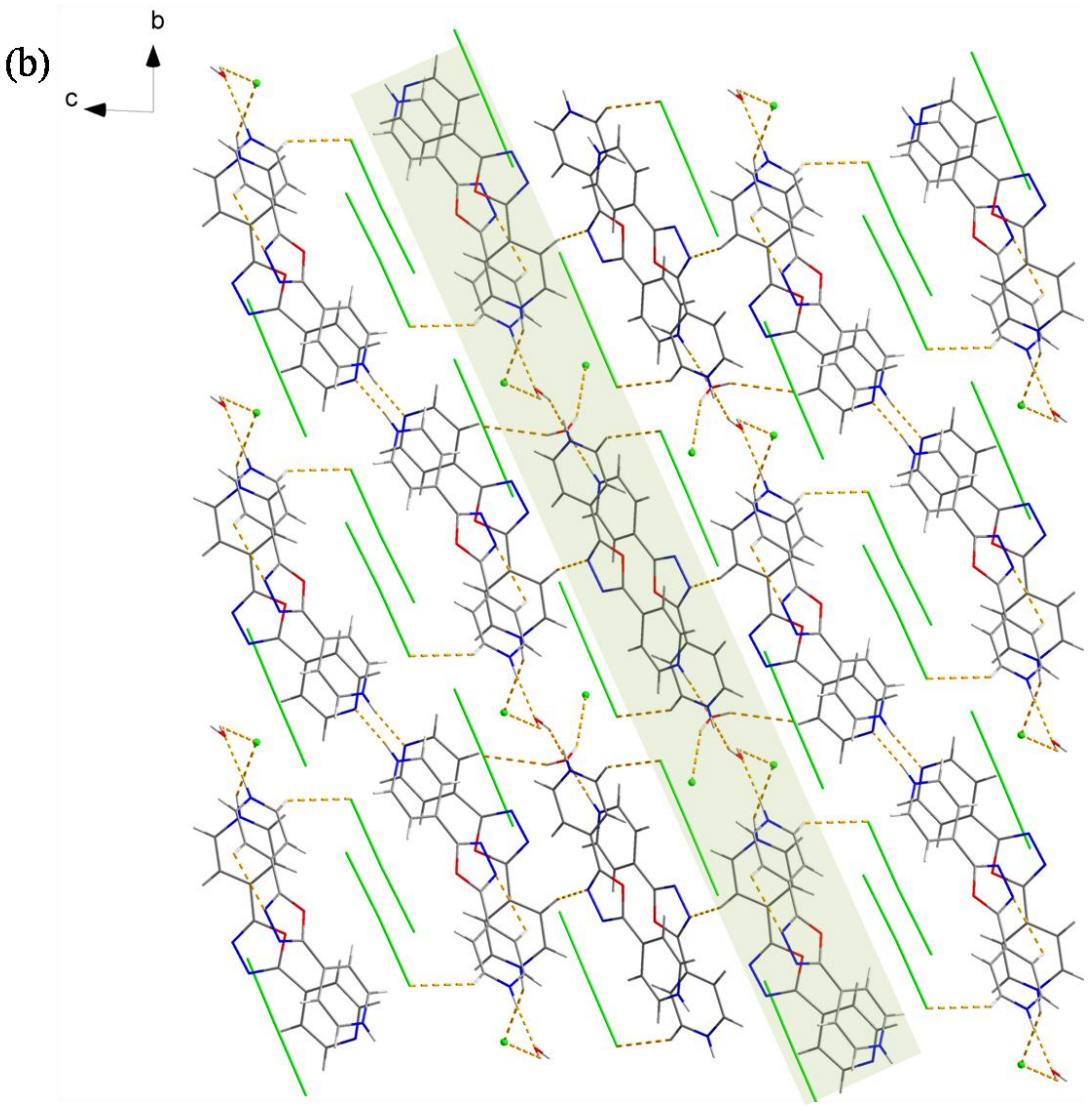

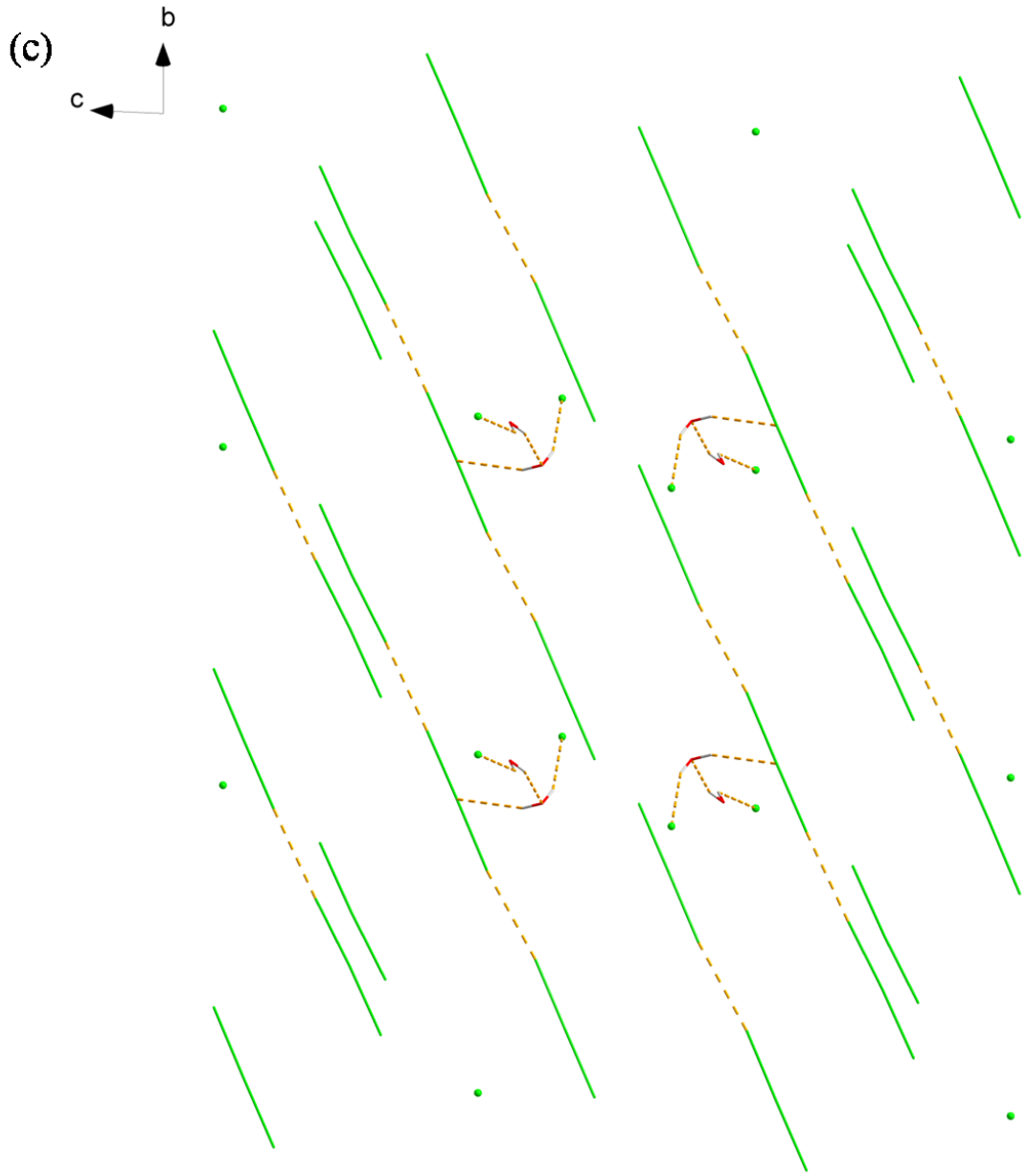

Fig. 3 (a) The coordination sphere of iodide anion in **3** where ball-and-stick model was used for I^- ions for clarity; (b) The 3D hydrogen-bonding network parallel to the *bc*-plane; (c) The structure with cations deleted through hydrogen bonds and short contacts. Hydrogen bonds and $\pi\cdots\pi$ interactions are represented by light orange and black dotted lines, respectively.

Besides the above X–H $\cdots$I (X = O, N, C) interactions, short I $\cdots$I contacts and $\pi\cdots\pi$ interactions, some hydrogen bonds not involved in iodide ions codetermine the supramolecular network, ranging from O–H $\cdots$O, N–H $\cdots$Y (Y = N, O) to C–H $\cdots$N (Fig. 3b). Declining cationic chains are surrounded by its bilateral linear I_3^- anions

while spherical I^- anions always accompany H_2O molecules and appear near the protonated pyridine rings. In order for better observation of the packing of iodine ions and water molecules, cations have been deleted as shown in Fig. 3c. Triiodides are in perfect alignment while I10 and I11 are hydrogen-bonded to two H_2O molecules, one of which is linked with I2 atom from the centre of the triiodide trimer producing an appealing subunit.

Packing parallel to the *ac*-plane, we can see that the supramolecular architecture is composed of independent substructures (Fig. S3b). Diprotonated 4-H_2bpo^{2+} cations alternate with monoprotonated 4-$Hbpo^+$ ones in the first and second layer and the two types of molecules show a certain inclination angle. Throughout the two adjacent layers, molecules of the same kind are arranged face to face with their diagonal ones. Somewhat differently, only diprotonated 4-H_2bpo^{2+} cations appear in the third layer and molecules in the ortho-position are antiparallel to each other. The above independent substructures appeal to us, one of which has been selected in the pale green background. As shown in Fig. S3c, the subunit was rotated a little with triiodide ions deleted, and then the side view was observed where bent chains are not connected with each other. Among them, the chain in pale green is viewed along the *c*-axis and three types of hydrogen-bonding ring motifs unfold before us, namely intramolecular S(5) and intermolecular large ring $R_{10}^6(36)$ as well as $R_8^6(56)$.

Structure description of compound 4.

Although it possesses the same triclinic space group $P\bar{1}$ as **3**, compound **4** exhibits quite a different structure. The molecular structure of **4** consists of two monoprotonated 4-$Hbpo^+$ cations, two octahedral PF_6^- anions and one H_2O molecule, where fluorine atoms are in disorder (Fig. 4a and Fig. S4a). 4-$Hbpo^+$ cations and PF_6^- anions are interlinked to each other through C–H···F hydrogen bonds (H···F, 2.41–2.51 Å; ∠C–H···F, 135–177°) and anion···π interactions (anion-centroid distance, 3.051–3.722 Å). Adjacent 4-$Hbpo^+$ cations interact with each other through hydrogen-bonding X–H···N (X = N, C) and π···π interactions with the distance of

3.418 Å.

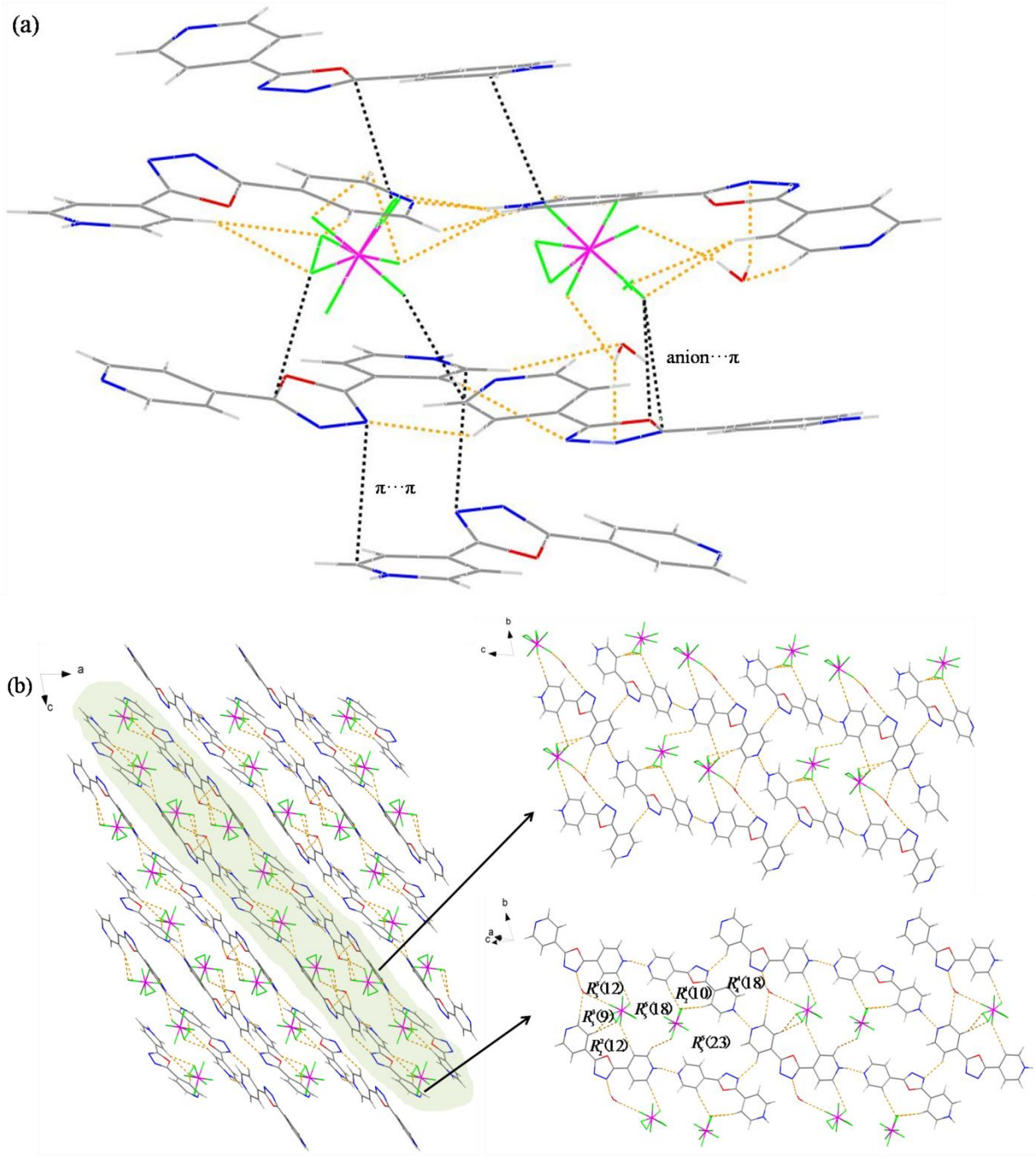

Fig. 4 (a) The coordination sphere of PF_6^- anion in **4**; (b) The 3D hydrogen-bonding network parallel to the *ac*-plane and the twin chains in pale green viewed along the *a*-axis. Hydrogen bonds are represented by light orange dashed lines while anion···π and π···π interactions are black.

These intermolecular interactions act as the driving force in the crystal packing. Running parallel to the *ac*-plane as shown in Fig. 4b, discrete chains are spread over

the whole space and the twin chains are antiparallel to each other where PF_6^- anions are sandwiched between them. Thereinto, such a pair of chains was chosen as the further study object in the pale green background. 2D supramolecular arrays appear before us on the right, which comprise multifarious ring motifs with graph set notation $R_3^3(9)$, $R_2^1(10)$, $R_2^2(12)$, $R_3^3(12)$, $R_4^4(18)$, $R_5^5(18)$ and $R_5^5(23)$. Packing parallel to the *ab*-plane (Fig. S4b), the supramolecular architecture seems terribly disorganized. In fact, 4-Hbpo$^+$ cations of random stacking circle relatively regular PF_6^- anions, just like the metal-organic frameworks (MOFs).

Structure description of compound 5.

For **5**, one bent dipyridine was diprotonated by two HBF_4 molecules and the coordination sphere of two tetrahedral BF_4^- anions has been illustrated in Fig. 5a. The three components (4-H_2bpo^{2+}–BF_4^-–H_2O) are closely connected to each other due to a wide variety of hydrogen bonds (O–H…F, N–H…X (X = O, F), C–H…Y (Y = N, F)), anion $\cdots\pi$ interactions and $\pi\cdots\pi$ interactions. They extend on the *ac*-plane to form a 3D supramolecular architecture, where cationic and ani onic layers emerge alternately and seem to be sandwiched by each other (Fig. 5b). In the 4-H_2bpo^{2+} layer, two cations of a pair are arrayed face to face and connected with another couple by the C12–H10 $\cdots$N3 hydrogen bond.

We find that BF_4^- ions in the anionic layer are packing like an independent scarecrow together with H_2O molecules, several of which resemble soldiers to stand in line (Fig. 5c). Such BF_4^- layer changes to two groups of discontinuous three-component substructures viewed along the *a*-axis so that we guess the above scarecrow-like structure may not be a unity. Indeed, two sets of symmetrical subunits are observed. Viewed along the *c*-axis, the V-shaped structures align, where H_2O molecule bridges the BF_4^- anions on both ends through the hydrogen-bonding interactions O2–H11 $\cdots$F4 and O2–H12 $\cdots$F5'. When stacking along the *a*-axis, the three components in staggered arrangement are weaved into a supramolecular framework, offering seven types of different hydrogen-bonding rings, *i.e.* $R_1^2(4)$,

$R_3^2(7)$, $R_2^2(10)$, $R_4^4(14)$, $R_4^4(15)$, $R_4^4(16)$ and $R_4^4(19)$ (Fig. S5b).

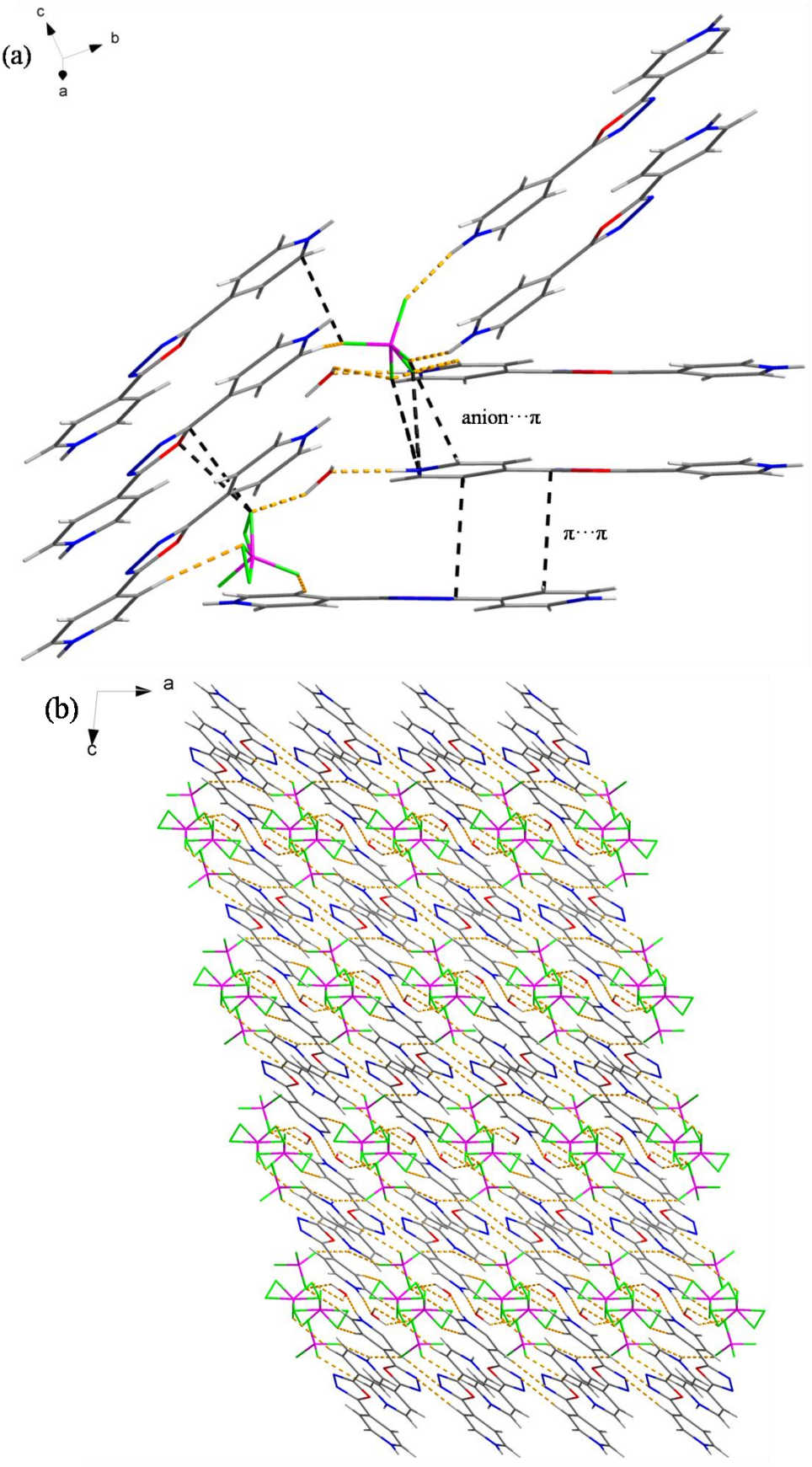

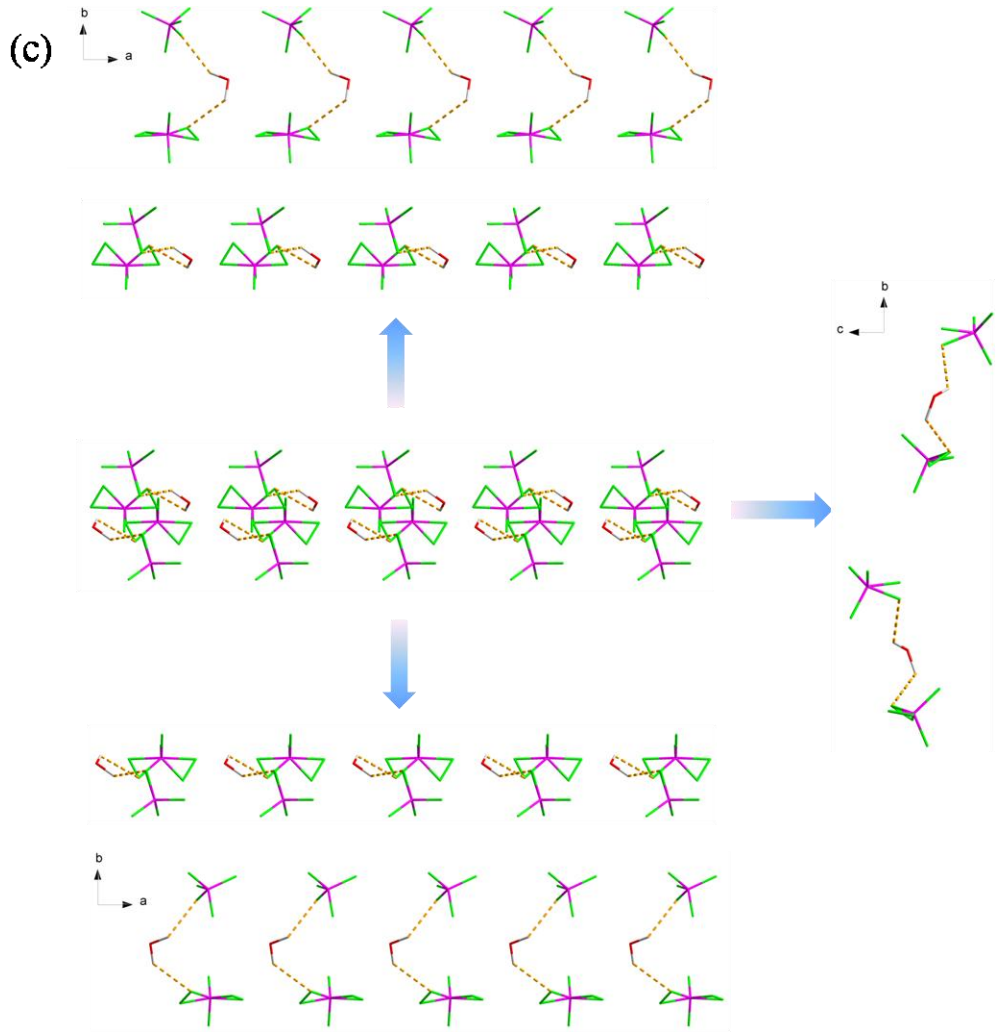

Fig. 5 (a) The coordination sphere of BF_4^- anion in **5**; (b) The 3D hydrogen-bonding network parallel to the *ac*-plane; (c) the BF_4^- anionic substructures. Hydrogen bonds are represented by light orange dashed lines while anion $\cdots\pi$ and $\pi\cdots\pi$ interactions are black.

Structure description of compound 6.

Although the same reactants were adopted in comparison with **5**, the different reaction ratio (1 : 1) and condition lead to disparate crystal structure and space group (triclinic *P*−1) in **6**. Structure determination revealed that one monoprotonated 4-Hbpo$^+$ cation counters one tetrahedral BF_4^- anion without disorder fluorine atom and protonated nitrogen atom comes from oxadiazole rather than pyridine, which is extremely rare for the coexistence of diazole and pyridine rings. Every BF_4^- anion attaches to nearby five 4-Hbpo$^+$ cations *via* the C–H $\cdots$F hydrogen bonds, anion $\cdots\pi$ and N–H $\cdots\pi$

interactions (Fig. 6a). It is worth mentioning that BF_4^- anions in **6** play a decisive role in the crystal packing since almost all hydrogen bonds take fluorine atoms as acceptors except the hydrogen bond C9–H5 ··N3. Specifically, their F2 and F4 atoms are employed to bridge two neighbouring columns of 4-$Hbpo^+$ cations through hydrogen-bonding interactions, facilitating the 3D supramolecular architecture (Fig. S6b).

Salt **6** just exhibits weak hydrogen-bonding interactions (C–H…N and C–H…F), anion ··π and N–H ··π interactions, but that does not impede the 3D supramolecular assembly. Running parallel to the *ac*-plane, 4-$Hbpo^+$ cations and BF_4^- anions locate alternately, producing a zigzag ribbon-like chain in the pale green background (Fig. 6b). From its side view on the right, the helical chain was observed and linked by BF_4^- anions. Weak C10–H6 ··F2 interactions help to maintain the linkage between these chains that align parallel to each other. Viewed along the *c*-axis, three types of hydrogen-bonding patterns are found to extend on the *ab*-plane, marked as $R_2^2(10)$, $R_4^2(12)$ and $R_4^4(32)$ (Fig. 6c).

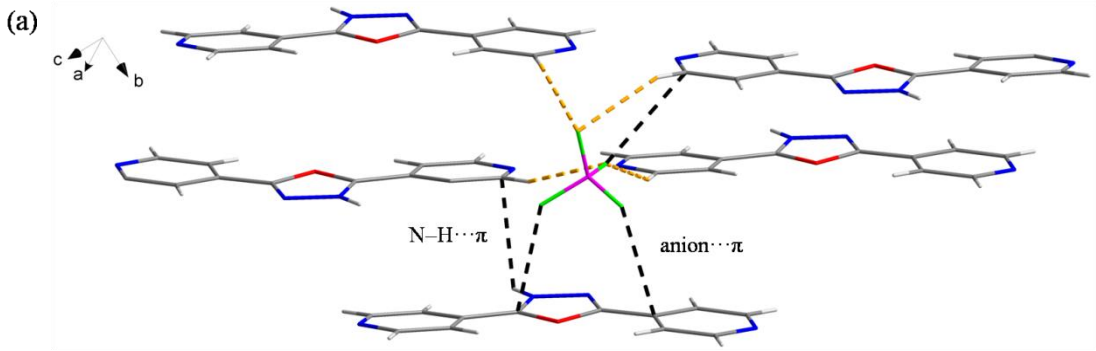

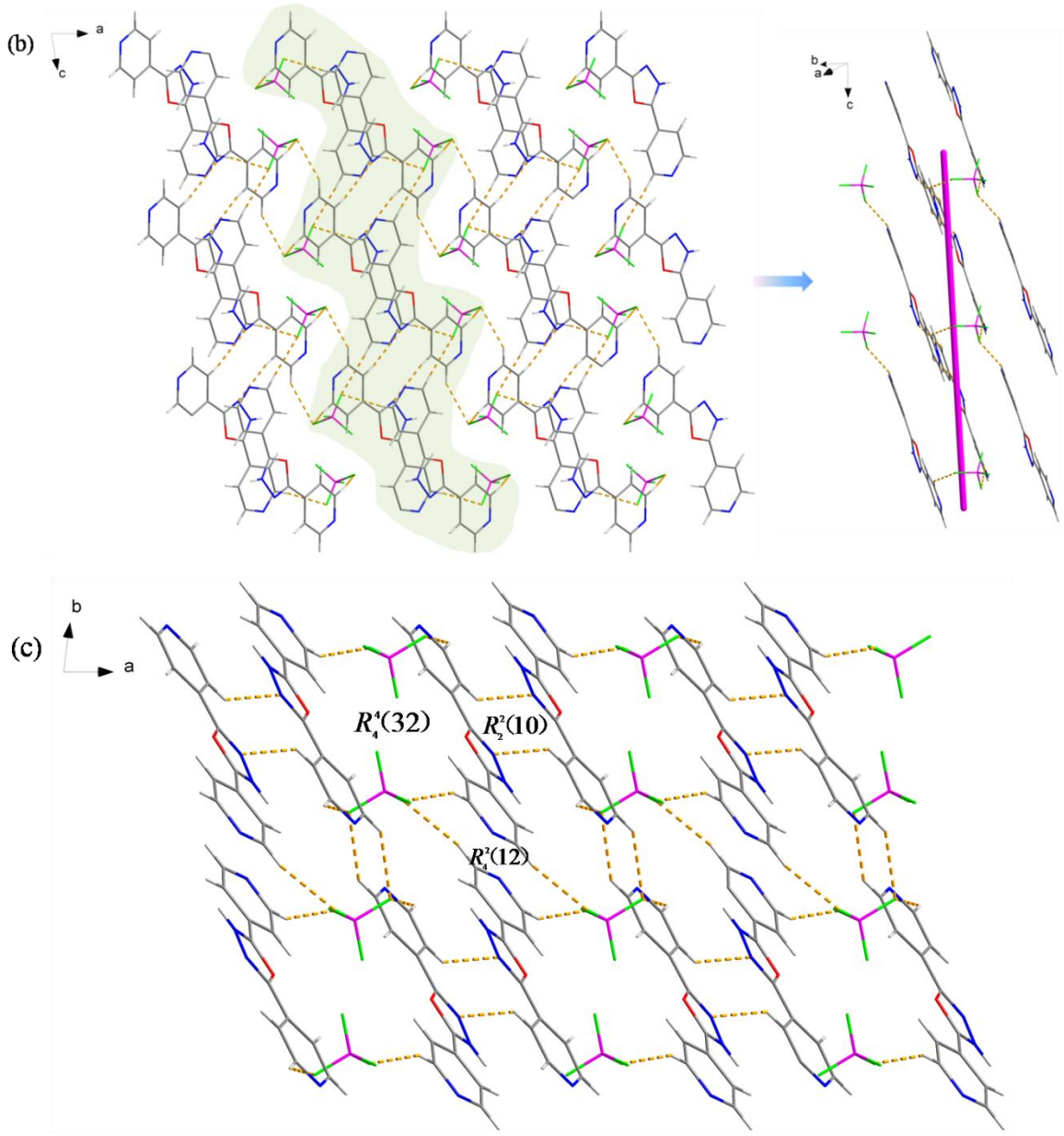

Fig. 6 (a) The coordination sphere of BF_4^- anion in **6**; (b) The 3D hydrogen-bonding network parallel to the *ac*-plane and the helical structure from the side view of the zigzag ribbon-like chain in the pale green background; (c) The 3D hydrogen-bonding network parallel to the *ab*-plane. Hydrogen bonds are represented by light orange dashed lines while anion $\cdots\pi$ and N–H $\cdots\pi$ interactions are black.

Structure description of compound 7.

Different from the above six salts, hydrothermal conditions induce the oxadiazole ring in 4-bpo to hydrolyze in situ during crystallization with H_2SO_4, yielding a new organic compound N,N′-bis(4-picolinoyl) hydrazine (4-bph). Salt **7** crystallizes in the

same space group $P2_1/c$ with **1** and one diprotonated 4-H_2bph^{2+} cation counterbalances one tetrahedral SO_4^{2-} anion in the asymmetric unit (Fig. S7a). Compared with the oxdiazole functional group in the above study, the amide (N–H) and carbonyl group (C=O) in 4-bph are strong hydrogen-bonding participators, which make it a more abundant hydrogen-bonding system.

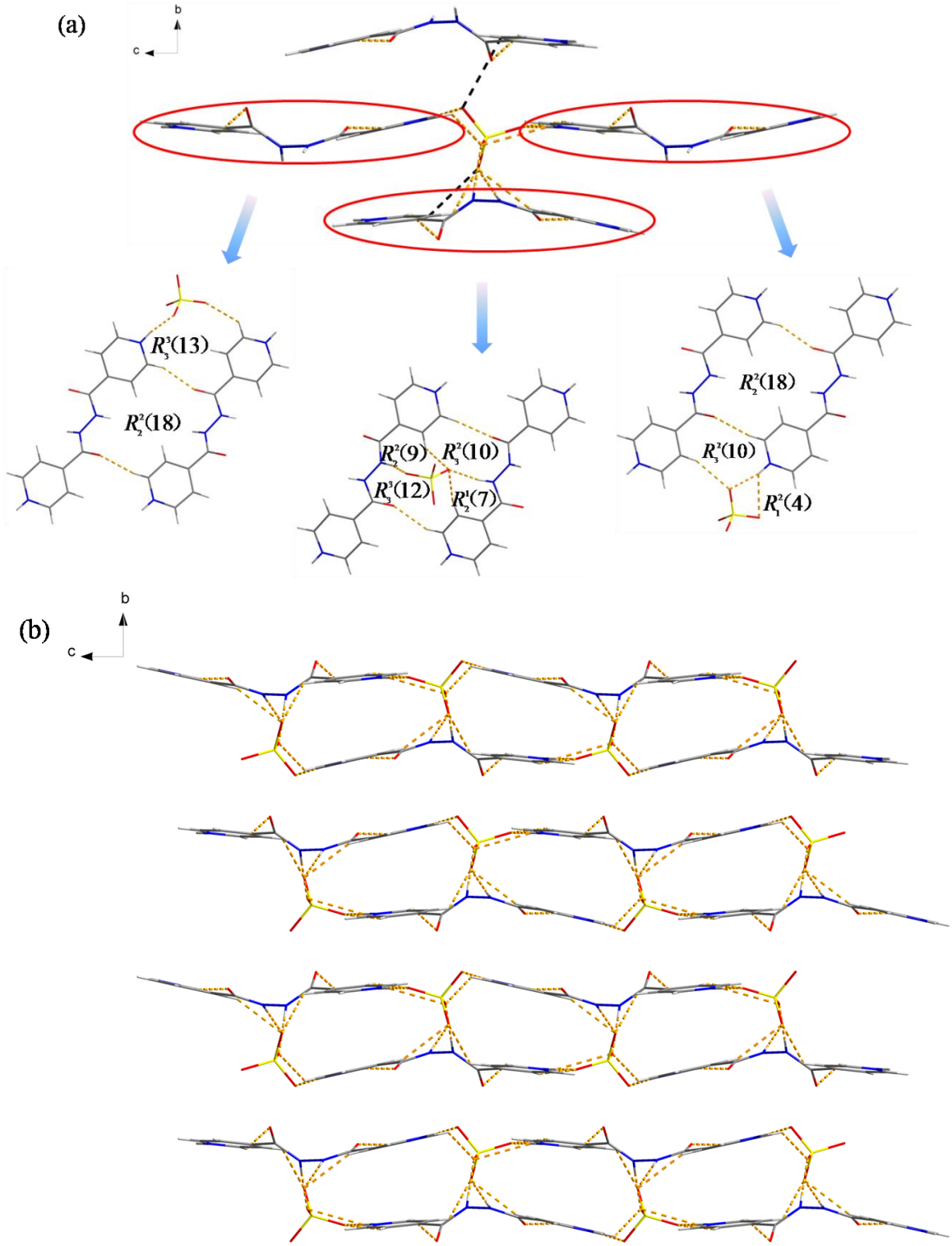

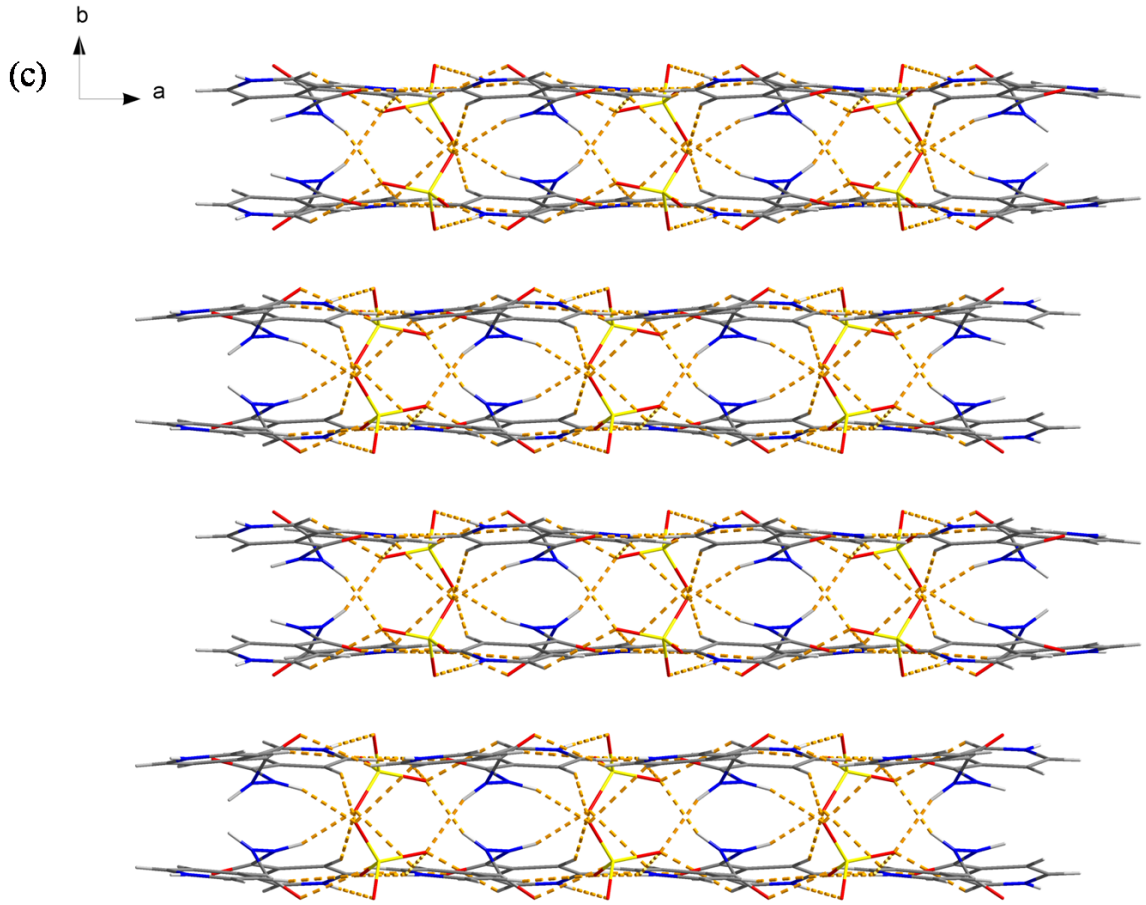

Fig. 7 (a) The coordination sphere of SO_4^{2-} anion in **7** and the perspective view of the subunit between one SO_4^{2-} anion and its surrounding 4-H_2bph^{2+} cations; (b) The 3D hydrogen-bonding network parallel to the *bc*-plane; (c) The 3D hydrogen-bonding network parallel to the *ab*-plane. Hydrogen bonds and anion$\cdots\pi$ interactions are represented by light orange and black dotted lines, respectively.

All oxygen atoms (O1–O6) are used as hydrogen-bonding acceptors, resulting in multifarious hydrogen bonds from strong N–H$\cdots$O to weak C–H$\cdots$O. Four oxygen atoms of SO_4^{2-} anion all participate in the formation of hydrogen bonds with its surrounding 4-H_2bph^{2+} cations, as shown in Fig. 7a. Among them, O4 and O5 atoms are bound to cations through anion$\cdots\pi$ interactions as well. Seven kinds of hydrogen-bonding motifs are generated with the graph-sets of $R_1^2(4)$, $R_2^1(7)$, $R_2^2(9)$, $R_3^2(10)$, $R_3^3(12)$, $R_3^3(13)$ and $R_2^2(18)$. Further analysis of the crystal packing indicates that grid-like ribbons or ladderlike chains are discrete and packing antiparallel to the

adjacent ones (Fig. 7b and Fig. 7c).

Structural diversity influenced by the inorganic anions

To explore the influence of inorganic anions on the angular dipyridine (4-bpo), we have obtained a series of supramolecular salts **1**–**7**, assisted by NO_3^-, HPO_4^{2-}, I_3^-/I^-, PF_6^-, BF_4^-, and SO_4^{2-}. Inorganic anions act as the dominant factor in the formation of supramolecular assemblies by impacting on the crystallization ratio, the protonated number and the final structures, which are attributed to their nature and geometry (spherical, linear, trigonal planar, tetrahedral and octahedral).

The detailed analysis of surrounding environment for anions has been carried out, where they all participate in the hydrogen-bonding interactions and anion$\cdots\pi$ interactions are widely utilized except salt **3**. With the assistance of water molecules, several anions result in appealing substructures. For instance, trigonal planar NO_3^- is interlinked to H_2O molecule in **1**, offering a wavelike chain. In **3**, linear triiodide trimers are generated by short I$\cdots$I contacts while two spherical iodine atoms are hydrogen-bonded to two H_2O molecules. The central I2 atom is bridged to one H_2O molecule, producing an appealing subunit. As for compound **5**, H_2O molecule is bound by two BF_4^- anions on both ends, forming the V-shaped structure that is packing to afford independent scarecrow-like substructures in line. In spite of no assist by water molecules, dimers arise from HPO_4^{2-} anions in **2** due to the coexistence of potential hydrogen-bonding donor and acceptor oxygen atoms.

In comparison, salts **4**, **6** and **7** do not maintain such close relationship with solvent water in appearance. Though compound **4** crystallizes together with H_2O, water molecules are locked nearby 4-Hbpo$^+$ cations through hydrogen-bonding interactions (O3–H20$\cdots$N3 and C2–H2$\cdots$O3), which may lower the possibility of anion-water substructures. When it comes to compounds **6** and **7**, hydrothermal conditions show control over the crystallization process without H_2O molecule, change the protonated site in **6** and the hydrolysis of 4-bpo in **7**.

Overall, these salts (**1**–**7**) exhibit various supramolecular architectures, a wide variety of hydrogen-bonding ring motifs and interesting substructures. From the view

of intermolecular interactions, hydrogen bonds (table S1) and weak forces (anion $\cdots\pi$ and $\pi\cdots\pi$ interactions, table S2) codetermine the whole crystal packing and show both competitive and complementary role in the formation of crystal structure. Once strong hydrogen bonds are quenched, the C–H bond is a little acidic in nature and can be used as a donor to interact with hydrogen-bonding acceptors. For example, weak hydrogen-bonding interactions (C–H$\cdots$F and C–H$\cdots$N) are exploited to construct supramolecular frameworks and BF_4^- anions facilitate the formation of helical chains in **6**.

In addition, two salts based on 4-bpo, $[(4\text{-}H_2bpo^{2+})(ClO_4^-)_2]\cdot H_2O$[44] and $[(4\text{-}H_2bpo^{2+})(Br^-)_2]\cdot H_2O$[45], have been reported previously. Structural analysis indicates that the former shows great similarity to compound **5** in the supramolecular networks, where V-shaped subunits are formed between ClO_4^- anion and H_2O molecule (Fig. S5b and Fig. S8). This may be accounted for similar tetrahedral ClO_4^- and BF_4^- anions. The latter bromide is the counterpart of salt **1**, in which 4-H_2bpo^{2+}cations are interweaved by spherical Br^- anions and water molecules to generate a similar wavelike chain (Fig. 1c and Fig. S9). Although **3** contains spherical I^- anions, bilateral linear I_3^- ions limit their activities.

It is clear from our present study that the nature and geometry of inorganic anions play a vital role in the crystal packing indeed. Crystal structures here provide a wealth of information about the rational design of inorganic anion-assisted supramolecular assemblies and the application of hydrogen bonds and weak forces in crystal engineering and supramolecular chemistry.

Conclusion

Seven ionic salts have been obtained by the self-assembly of bent dipyridyl 4-bpo, assisted by different inorganic anions (NO_3^-, HPO_4^{2-}, I_3^-/I^-, PF_6^-, BF_4^-, and SO_4^{2-}). 3D supramolecular architectures are observed in **1**, **2**, **5**, **6** but discrete structures in **3**, **4**, **7**. Such anions can effectively influence supramolecular architectures through extensive intermolecular interactions, ranging from hydrogen bonds, anion $\cdots\pi$ to $\pi\cdots\pi$ interactions. The examples here should help to develop supramolecular

assemblies assisted by anions and expand the understanding of the vital role of anions in the construction of supermolecules. Additionally, our research here allows us to better understand both competitive and complementary effects between strong hydrogen bonds and weak interactions in the crystal engineering and supramolecular chemistry.

Acknowledgements

We gratefully acknowledge financial support from the Natural Science Foundations of China (51173082), from Jiangsu Province and PAPD (13KJB150028, BM2012010, BK20141425 and YX03001) and Program for Postgraduates Research Innovation in University of Jiangsu Province (CXZZ12-0456).

References

1 J. L. Sessler, P. A. Gale and W. S. Cho, *Anion receptor chemistry*, Royal Society of Chemistry, 2006.

2 P. A. Gale, *Acc. Chem. Res.*, 2006, 39, 465-475.

3 P. A. Gale, S. E. Garcá-Garrido and J. Garric, *Chem. Soc. Rev.*, 2008, 37, 151-190.

4 J. Pérez and L. Riera, *Chem. Soc. Rev.*, 2008, 37, 2658-2667.

5 J. W. Steed, *Chem. Soc. Rev.*, 2009, 38, 506-519.

6 Z. Zhang and P. R. Schreiner, *Chem. Soc. Rev.*, 2009, 38, 1187-1198.

7 Y. Hua and A. H. Flood, *Chem. Soc. Rev.*, 2010, 39, 1262-1271.

8 S. O. Kang, J. M. Llinares, V. W. Day and K. Bowman-James, *Chem. Soc. Rev.*, 2010, 39, 3980-4003.

9 R. Custelcean, in *Constitutional Dynamic Chemistry*, ed. M. Barboiu, Springer-Verlag Berlin, Berlin, 2012, 322, 193-216.

10 A. Caballero, F. Zapata and P. D. Beer, *Coord. Chem. Rev.*, 2013, 257, 2434-2455.

11 R. Custelcean, *Chem. Soc. Rev.*, 2010, 39, 3675-3685.

12 Z. Y. Zhang, Z. P. Deng, L. H. Huo, H. Zhao and S. Gao, *Crystengcomm*, 2013, 15, 5261-5274.

13 P. D. Beer and P. A. Gale, *Angew. Chem.-Int. Edit.*, 2001, 40, 486-516.

14 N. Gimeno and R. Vilar, *Coord. Chem. Rev.*, 2006, 250, 3161-3189.

15 M. S. Vickers and P. D. Beer, *Chem. Soc. Rev.*, 2007, 36, 211-225.

16 M. D. Lankshear and P. D. Beer, *Acc. Chem. Res.*, 2007, 40, 657-668.

17 R. Vilar, in *Recognition of Anions*, ed. R. Vilar, Springer-Verlag Berlin, Berlin, 2008, 129, 175-206.

18 R. Vilar, *Eur. J. Inorg. Chem.*, 2008, 357-367.

19 R. Custelcean, D.-e. Jiang, B. P. Hay, W. Luo and B. Gu, *Cryst. Growth Des.*, 2008, 8, 1909-1915.

20 K. Uzarevic, I. Dilovic, N. Bregovic, V. Tomisic, D. Matkovic-Calogovic and M. Cindric, *Chem.-Eur. J.*, 2011, 17, 10889-10897.

21 G. T. Spence and P. D. Beer, *Acc. Chem. Res.*, 2013, 46, 571-586.

22 L. A. Joyce, S. H. Shabbir and E. V. Anslyn, *Chem. Soc. Rev.*, 2010, 39, 3621-3632.

23 J. L. Gulbransen and C. M. Fitchett, *Crystengcomm*, 2012, 14, 5394-5397.

24 H. T. Chifotides, B. L. Schottel and K. R. Dunbar, *Angew. Chem.-Int. Edit.*, 2010, 49, 7202-7207.

25 H. T. Chifotides and K. R. Dunbar, *Acc. Chem. Res.*, 2013, 46, 894-906.

26 A. Caballero, F. Zapata, L. Gonzalez, P. Molina, I. Alkorta and J. Elguero, *Chem. Commun.*, 2014, 50, 4680--4682.

27 P. Gamez, *Inorg. Chem. Front.*, 2014, 1, 35-43.

28 C. Jia, B. Wu, S. Li, Z. Yang, Q. Zhao, J. Liang, Q.-S. Li and X.-J. Yang, *Chem. Commun.*, 2010, 46, 5376-5378.

29 C. Jia, B. Wu, S. Li, X. Huang and X.-J. Yang, *Org. Lett.*, 2010, 12, 5612-5615.

30 C. Jia, B. Wu, S. Li, X. Huang, Q. Zhao, Q. S. Li and X. J. Yang, *Angew. Chem.-Int. Edit.*, 2011, 50, 486-490.

31 S. G. Li, C. D. Jia, B. Wu, Q. Luo, X. J. Huang, Z. W. Yang, Q. S. Li and X. J. Yang, *Angew. Chem.-Int. Edit.*, 2011, 50, 5720-5723.

32 Z.-P. Deng, H.-L. Qi, L.-H. Huo, H. Zhao and S. Gao, *Crystengcomm*, 2011, 13, 6632-6642.

33 R. Li, Y. Zhao, S. Li, P. Yang, X. Huang, X.-J. Yang and B. Wu, *Inorg. Chem.*,

2013, 52, 5851-5860.

34 B. Wu, F. J. Cui, Y. B. Lei, S. G. Li, N. D. Amadeu, C. Janiak, Y. J. Lin, L. H. Weng, Y. Y. Wang and X. J. Yang, *Angew. Chem.-Int. Edit.*, 2013, 52, 5096-5100.

35 T.-P. Liu, L.-H. Huo, Z.-P. Deng, H. Zhao and S. Gao, *RSC Adv.*, 2014, 4, 40693-40710.

36 P. A. Gale, W. Dehaen and E. Alcade, *Anion Recognition in Supramolecular Chemistry*, Springer, 2010.

37 M. Arunachalam and P. Ghosh, *Chem. Commun.*, 2011, 47, 8477-8492.

38 X. H. Ding, Y. H. Li, S. Wang, X. A. Li and W. Huang, *J. Mol. Struct.*, 2013, 1051, 124-131.

39 M. Du, Z. H. Zhang, X. J. Zhao and H. Cai, *Cryst. Growth Des.*, 2006, 6, 114-121.

40 M. Du, Z.-H. Zhang and X.-J. Zhao, *Cryst. Growth Des.*, 2005, 5, 1199-1208.

41 M. Du, Z.-H. Zhang and X.-J. Zhao, *Cryst. Growth Des.*, 2005, 5, 1247-1254.

42 M. Du, Z.-H. Zhang and X.-J. Zhao, *Cryst. Growth Des.*, 2006, 6, 390-396.

43 L. Wang, L. Zhao, Y. J. Hu, W. Q. Wang, R. X. Chen and Y. Yang, *Crystengcomm*, 2013, 15, 2835-2852.

44 Y.-T. Wang, G.-M. Tang, D.-W. Qin, H.-D. Duan and S. W. Ng, *Acta Crystallogr. Sect. E.*, 2006, 62, O3094-O3095.

45 M. T. Han and Y. Zhang, *Acta Crystallogr. Sect. E.*, 2010, 66, O3212-U1031.

46 M. Kubicki and P. W. Codding, *Acta Crystallogr. Sect. E.*, 2001, 57, o122-o124.

47 F. Bentiss and M. Lagrenee, *J. heterocycl. chem.*, 1999, 36, 1029-1032.